AN EXPERIMENTAL INVESTIGATION OF TECHNIQUES
TO SUPPRESS EDGETONES FROM PERFORATED
WIND TUNNEL WALLS

PROPULSION WIND TUNNEL FACILITY
ARNOLD ENGINEERING DEVELOPMENT CENTER
AIR FORCE SYSTEMS COMMAND
ARNOLD AIR FORCE STATION, TENNESSEE 37389

August 1975

Final Report for Period September 19, 1972 to December 20, 1974

Approved for public release; distribution unlimited.

Prepared for

ARNOLD ENGINEERING DEVELOPMENT CENTER (DY)
AIR FORCE SYSTEMS COMMAND
ARNOLD AIR FORCE STATION, TENNESSEE 37389

NOTICES

When U. S. Government drawings specifications, or other data are used for any purpose other than a definitely related Government procurement operation, the Government thereby incurs no responsibility nor any obligation whatsoever, and the fact that the Government may have formulated, furnished, or in any way supplied the said drawings, specifications, or other data, is not to be regarded by implication or otherwise, or in any manner licensing the holder or any other person or corporation, or conveying any rights or permission to manufacture, use, or sell any patented invention that may in any way be related thereto.

Qualified users may obtain copies of this report from the Defense Documentation Center.

References to named commercial products in this report are not to be considered in any sense as an endorsement of the product by the United States Air Force or the Government.
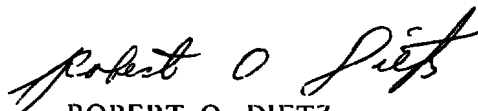
APPROVAL STATEMENT

This technical report has been reviewed and is approved for publication.

FOR THE COMMANDER

CARLOS TIRRES
Captain, USAF
Research & Development
    Division
Directorate of Technology

ROBERT O. DIETZ
Director of Technology

REPORT DOCUMENTATION PAGE		READ INSTRUCTIONS BEFORE COMPLETING FORM
1. REPORT NUMBER AEDC-TR-75-88	2 GOVT ACCESSION NO.	3. RECIPIENT'S CATALOG NUMBER
4. TITLE *(and Subtitle)* AN EXPERIMENTAL INVESTIGATION OF TECHNIQUES TO SUPPRESS EDGETONES FROM PERFORATED WIND TUNNEL WALLS		5 TYPE OF REPORT & PERIOD COVERED Final Report—September 19, 1972 to December 20, 1974
		6. PERFORMING ORG. REPORT NUMBER
7. AUTHOR(s) N. S. Dougherty, Jr., C. F. Anderson, and R. L. Parker, Jr., ARO, Inc.		8. CONTRACT OR GRANT NUMBER(s)
9 PERFORMING ORGANIZATION NAME AND ADDRESS Arnold Engineering Development Center (DY) Arnold Air Force Station, Tennessee 37389		10. PROGRAM ELEMENT, PROJECT, TASK AREA & WORK UNIT NUMBERS Program Element 65807F
11 CONTROLLING OFFICE NAME AND ADDRESS Arnold Engineering Development Center (DYFS) Arnold Air Force Station, Tennessee 37389		12. REPORT DATE August 1975
		13. NUMBER OF PAGES 37
14 MONITORING AGENCY NAME & ADDRESS(if different from Controlling Office)		15. SECURITY CLASS. (of this report) UNCLASSIFIED
		15a. DECLASSIFICATION/DOWNGRADING SCHEDULE N/A

16 DISTRIBUTION STATEMENT (of this Report)

Approved for public release; distribution unlimited.

17 DISTRIBUTION STATEMENT (of the abstract entered in Block 20, if different from Report)

18 SUPPLEMENTARY NOTES

Available in DDC

19 KEY WORDS (Continue on reverse side if necessary and identify by block number)

test methods	walls (perforated)	supersonic flow
suppression	transonic flow	
noise (aerodynamic)	resonance	
wind tunnels	Mach number	

20 ABSTRACT (Continue on reverse side if necessary and identify by block number)

The aerodynamic noise emitted by perforated walls in transonic wind tunnels has been under study for several years at AEDC. This report presents a summary of recent experimental tests at the Propulsion Wind Tunnel Facility (PWT) in the 6-In. Acoustic Research Tunnel (ART) on ways to suppress perforated wall noise in transonic test sections. The mechanism of noise generation from perforated walls having 60-deg inclined holes is the edgetone

DD ₁ FORM ₇₃ 1473   EDITION OF 1 NOV 65 IS OBSOLETE

20. ABSTRACT (Continued)

phenomenon where the shear layer over each hole interacts with the trailing edge to produce intense tones at discrete frequencies. Suppression of the edgetone generation mechanism is required if the noise is to be reduced. Noise reduction by factors of four to six was achieved with several modified wall samples in the 6-in. tunnel at resonance conditions. Feasibility of the modification selected for actual transonic tunnel test sections was demonstrated using properly scaled hardware in the 1-Ft Transonic Tunnel (Aerodynamic Wind Tunnel, Transonic (1T)) at AEDC.

AFSC
Arnold AFS Tenn

PREFACE

CONTENTS

ILLUSTRATIONS

TABLES

1.0 INTRODUCTION

There is a growing awareness in aerodynamic testing that the aero-acoustic environment in conventional wind tunnel test sections is influencing test results. An increased emphasis has, therefore, been placed on attempting to define levels and origin of acoustic disturbances and to quantify their effects on various types of testing. Numerous acoustic studies (Refs. 1, 2, and 3), for example, have provided measurements of background pressure fluctuations in various wind tunnels. A criterion using such measurements was advanced by Mabey (Ref. 4) for maximum acceptable disturbance levels in subsonic and transonic facilities if adequate prediction of aircraft buffet boundaries is to be made. Model boundary-layer transition Reynolds number (Ref. 5) is also being used to indicate Reynolds number effects from acoustic disturbances in wind tunnel flow which might affect basic lift, drag, and pitching-moment data. Of particular concern are transonic flows that have large separation zones and significant shock/boundary-layer interactions.

Ironically, transonic wind tunnels have been found to contain the highest acoustic disturbances of any type wind tunnel. The high-amplitude noise is a direct result of the requirement to vent a transonic test section to a surrounding plenum chamber in order to establish transonic flows. There are three continuous flow transonic tunnels at the Arnold Engineering Development Center (AEDC). Maximum overall noise levels measured in the test sections of each are shown in Table 1. Each of these tunnels has a test section formed of perforated walls with uniformly distributed holes. The holes are inclined at an angle of 60 deg, which gives them a differential resistance between inflow and outflow. One or more discrete whistling tones are emitted by the array of holes. Tone frequencies increase with increasing tunnel Mach number, and the tones attain maximum amplitude at a particular resonant Mach number. These tones, which have been found to exhibit characteristics similar to classical edgetones (Refs. 6 and 7), dominate the test section noise spectra by as much as 20 db over background random noise components and raise the overall noise levels by as much as 10 db.

The aerodynamic noise emitted by the perforated walls has been under study for several years at AEDC. A recently concluded experimental study was performed in a specially constructed, low-noise Acoustic Research Tunnel (ART) which has a 6-in. test section. The

objective of the study was to perform an investigation of the acoustic parameters associated with perforated walls used at AEDC which might lead to design criteria for the reduction of wall-generated noise and improvement of test section flow quality. Suppression of the edgetone generation mechanism is required if the noise is to be reduced. This required some modification to each hole. The selection of a suitable modification scheme, therefore, became the object of the experimental investigation and is the subject of this report.

Table 1. Maximum Test Section Noise Levels in the AEDC Transonic Tunnels

Tunnel	Sound Pressure Level, db (Re 0.0002 dynes/cm^2)
Propulsion Wind Tunnel (16T)	152
Aerodynamic Wind Tunnel (4T)	152
Aerodynamic Wind Tunnel (1T)	160

2.0 PERFORATED WALLS

The hole pattern used in Propulsion Wind Tunnel (16T) evolved from a series of developmental tests in Aerodynamic Wind Tunnel (1T) during the 1950's which are described by Pindzola and Chew (Ref. 8) and by Goethert (Ref. 9). The holes were arranged to give a uniform wall porosity, τ, of six percent. The sizing of the holes is a function of tunnel wall boundary-layer thickness using criteria suggested by Lukasiewicz (Ref. 10). Inclination of hole angle to 60 deg in conjunction with six-percent porosity resulted from an optimization to provide cancellation at the wall of both shock and expansion waves from test models, thereby minimizing the interference to the model flow field at low supersonic speeds.

Actual samples of perforated walls from the three transonic tunnels were tested in the 6-in. ART so that there could be no question about wall impedance matching. A photograph of the basic wall samples tested is presented in Fig. 1. Cross-sectional details are shown in Fig. 2.
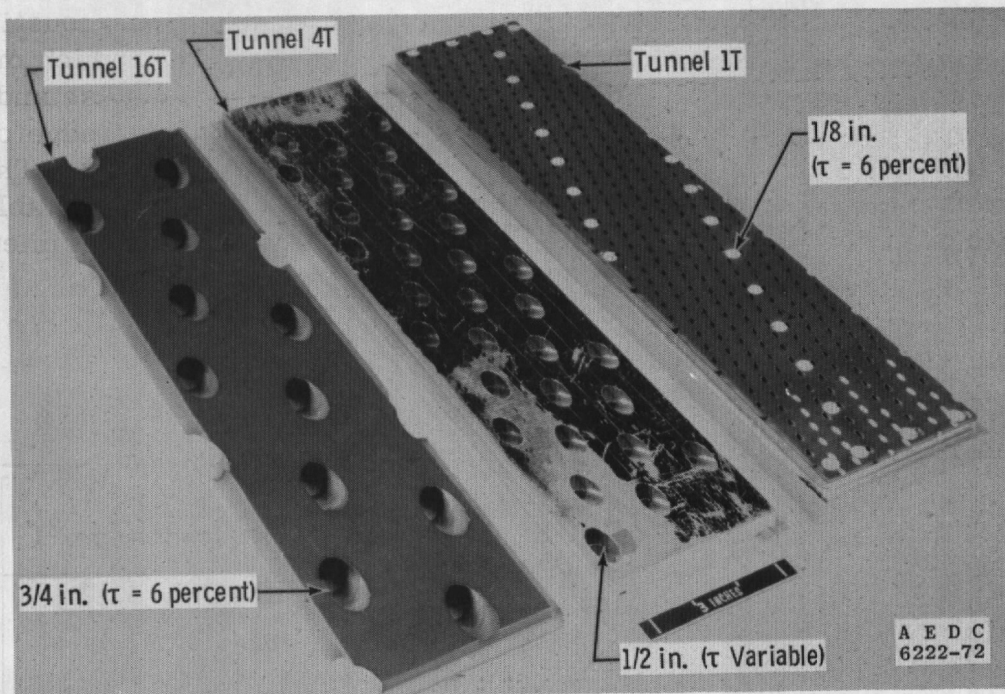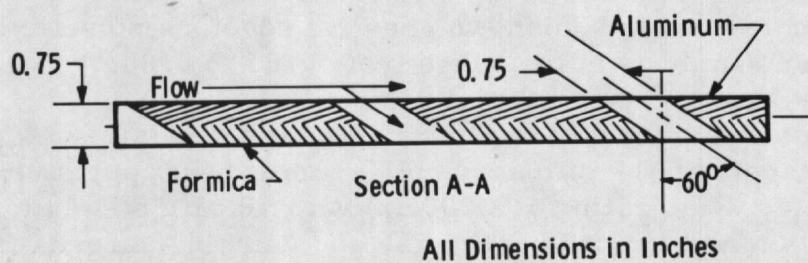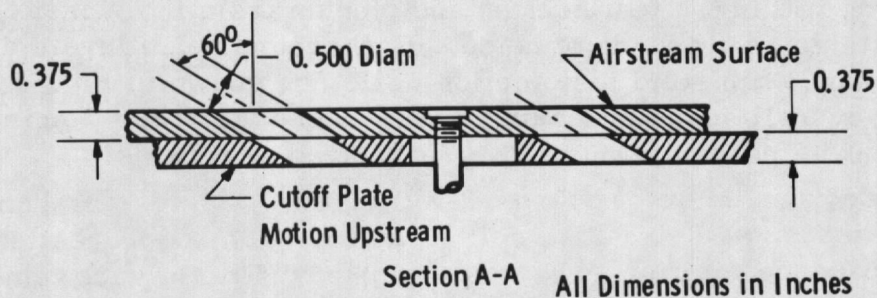
6

Figure 1. Perforated wall samples.

a. Tunnel 16T perforated walls

b. Tunnel 4T perforated walls
Figure 2. Cross sections of Tunnels 16T and 4T perforation design.

7

The walls from Tunnels 16T and 1T have fixed six-percent porosity with hole diameters of 3/4 and 1/8 in., respectively. Hole diameter in the Aerodynamic Wind Tunnel (4T) walls is 1/2 in. with variable porosity. The wall materials are aluminum backed by formica (one-half thickness) in Tunnel 16T, double-plate aluminum with a sliding backup plate to provide a variable porosity feature in Tunnel 4T, and micarta in Tunnel 1T. Reduction of the porosity at Mach numbers between 1.0 and 1.2 in Tunnel 4T gives improved wall interference characteristics (Ref. 11). In all three tunnels, plenum suction is applied to the walls in proper combination with small wall divergence angles to control the axial-pressure distribution for constant Mach number throughout the test region. Depending upon the model blockage area/tunnel cross-section area ratio, plenum suction for wall boundary-layer control is usually applied at approximately Mach number 0.7 and above.

3.0 ACOUSTIC RESEARCH TUNNEL

The 6-in. ART is a continuous flow, atmospheric indraft tunnel capable of being operated from Mach number 0.1 to 1.1. This Mach number range was sufficient for the present study because experience in the full-scale tunnels had shown greatest edgetone noise to occur at resonant Mach numbers in the range from 0.65 to 0.85.

A schematic diagram of the tunnel is presented in Fig. 3. The acoustic silencers in the diffuser and plenum exhaust ducts (46-db maximum attenuation rating at 1,200 Hz) with vibration isolation expansion joints together with honeycomb and damping screens in the intake provided a relatively low background noise level for these experiments. The exhaust machinery is located well remote from the tunnel. These features allowed the isolation of noise phenomena occurring within the test section and plenum from the tunnel drive control systems as a source of noise. Background noise levels attained in the tunnel with solid test section walls are shown in Fig. 4 in the form of overall sound pressure level. These were at a nominal ΔC_p level of 0.45 percent, where ΔC_p is derived as follows:

$$\Delta C_p = \frac{\widetilde{P}_{rms}}{q_\infty} \times 100, \text{ percent} \tag{1}$$
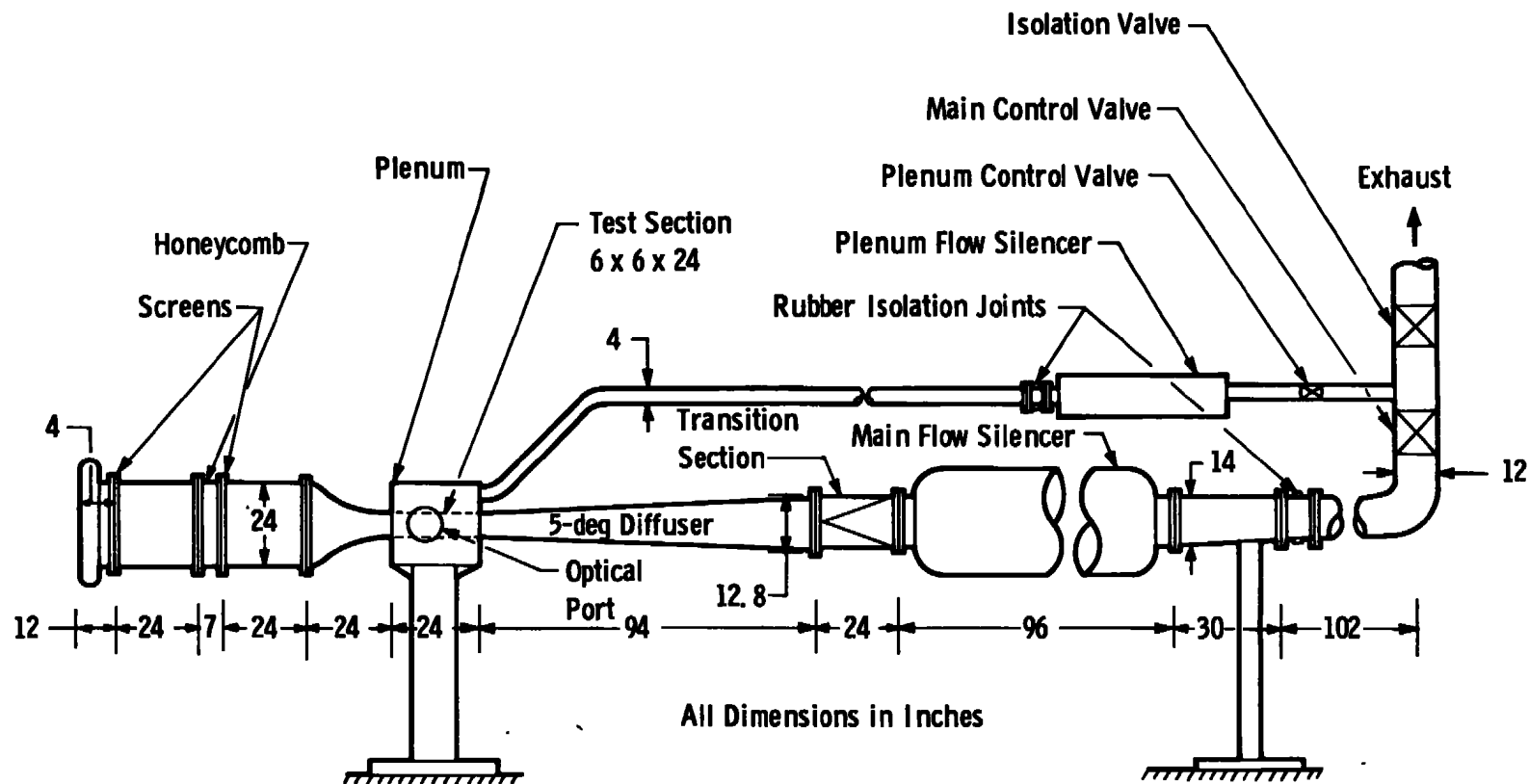
Figure 3. Acoustic Research Tunnel (ART).
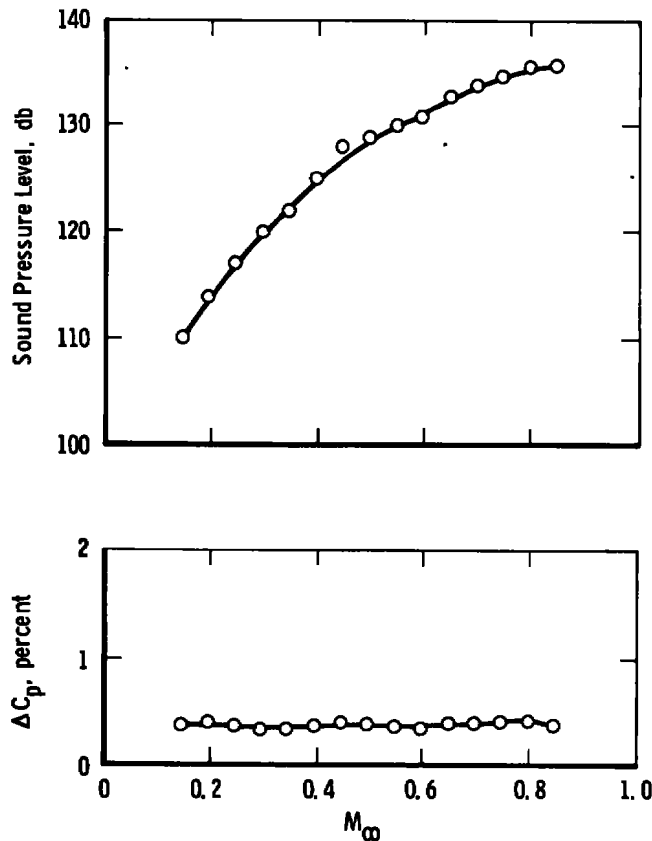
Figure 4. Results of ART background noise calibration.

Here, $\tilde{p}_{rms}$ is the time-averaged, frequency-integrated fluctuating pressure (overall sound pressure level) measured by a microphone in a frequency band from approximately 10 Hz to approximately 20 kHz. A level of $\Delta C_p = 0.45$ percent corresponds closely to the expected level of sound radiation from a turbulent boundary layer on the test section walls in the range of Reynolds numbers attained with atmospheric total pressure and temperature. (See Ref. 12, for example.)

Two 1/4-in.-diam Bruel and Kjaer condenser-type microphones were used to record the sound pressure level, $\tilde{p}_{rms}$. One microphone was flush-mounted on the test section sidewall, and the other was placed in the plenum chamber. The output of each microphone was recorded on a true-root-mean-square voltmeter with 1-sec time-constant using 5-sec minimum averaging time. The data were also recorded on an FM magnetic tape system using 10-kHz frequency response for spectral analysis. The microphones were calibrated by

direct application of a 140-db sound pressure level at 1-kHz frequency using a pistonphone with ±0.5-db certified accuracy.

A spark schlieren system with an 8-in.-diam field of view and a 2-μsec pulse illumination was used for viewing the boundary-layer phenomena at the bottom wall and the far field wave propagation phenomena across the test section. The schlieren data obtained provided the needed verification of the wall noise generation and propagation mechanisms.

4.0 EXPERIMENTAL TECHNIQUE

The experimental technique was to obtain first the baseline noise level data for each wall sample in the 6-in. ART and then to perform cut-and-try type testing of various modification schemes to evaluate the degree of noise reduction that could be obtained. A goal of 10 db (or a factor exceeding three) was arbitrarily chosen to be the minimum acceptable degree of noise reduction, this goal being applied to worst-case resonance conditions occurring over the Mach number range of tunnel operation.

The basic test procedure was to perform Mach number variations from approximately 0.3, where edgetones generally first appeared, to the maximum obtainable with a given set of wall samples. Tests were performed first on a single wall sample using a solid opposing wall and then with top and bottom opposing wall samples. With a single sample (in the bottom wall), the choking Mach number was generally near 0.88. With opposing wall samples, the Mach number could be increased to about 1.1.

Wall suction weight flow in combination with wall divergence angle was treated as a secondary variable in the experiment. In all cases, wall static pressures on the test section solid side wall were monitored in order to choose a combination of plenum suction flow and wall angle that gave a reasonably flat axial Mach number distribution throughout the test section.

An essentially constant inlet boundary-layer thickness was provided for each wall sample in the 6-in. ART. A typical velocity profile obtained at Mach number 0.5 on a solid bottom wall insert in place of a perforated wall sample 3 in. downstream of the throat is shown in

Fig. 5. After verification that the noise mechanism occurring from the three types of wall samples in the ART was the same as that which occurs in the full-scale tunnels, testing with nonscale boundary-layer thickness was considered to be of little consequence for evaluation of effectiveness of a particular noise suppression device.

with chart annotations:

$\delta^* = 0.0364$ in.
$\delta = 0.288$ in.
Re/ft $= 3.22 \times 10^6$
$M_\infty = 0.5$

Y-axis: U/U_∞
X-axis: Distance from Wall, in.
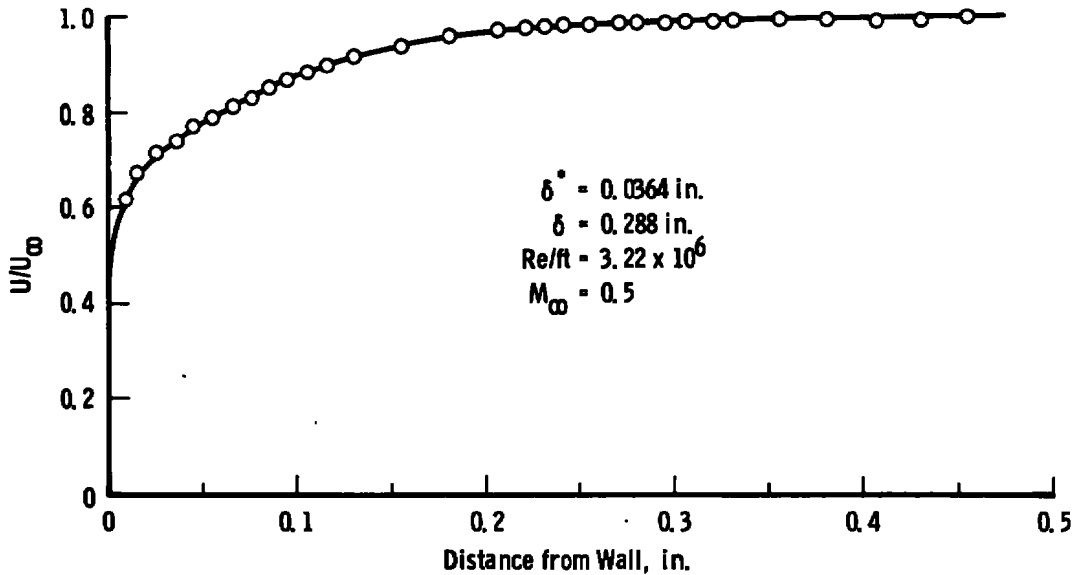
Figure 5. Typical boundary-layer velocity profile in the ART test section.

From the analysis of the baseline wall sample data, the judgment was made that effective suppression of the noise from the perforated walls would require some modification to each hole. The design philosophy established for the hole modification was based on the practical and economic constraints (1) that the modification selected should result in a minimal change to the basic wall configuration (i.e., it should be a simple hole geometry modification that would not necessitate redesign of the entire wall) and (2) that this modification should not significantly alter the wall crossflow characteristics to the extent that it would compromise the favorable transonic performance of the wall.

5.0 THE NOISE GENERATION MECHANISM

Fundamental to an aerodynamic whistling mechanism is the conversion of a small disturbance in a flow stream into a large one through

instability of the stream. The basic elements of such a system are (1) a means of amplification and (2) a means of feeding part of the amplified energy back upstream to sustain and control the process. This analogy was applied to the shear layer occurring over 60-deg inclined holes in the airstream surface by Woolley and Karamcheti (Ref. 13).

The best analysis that appears to apply to 60-deg inclined holes is the semi-empirical analysis of cavity flows advanced by Rossiter (Ref. 14). Rossiter argued that at time $t = 0$, an identified phase of acoustic radiation leaves the trailing edge of the cavity and a vortex is at $\gamma_v \lambda_v$ behind the trailing edge (see Fig. 6). At the time $t = t'$, an identified phase of acoustic radiation arrives at the leading edge just as a vortex is shed. The vortex pattern has moved downstream a distance $kU_\infty t'$ in this time interval such that

$$m_v \lambda_v = h + \gamma_v \lambda_v + kU_\infty t' \tag{2}$$

where h is the axial distance between leading and trailing edges of the cavity. In the same time interval, the internal wave system has moved a distance ct' so that

$$h = m_A \lambda_A + ct' \tag{3}$$

Eliminating t' and substituting for λ_A and λ_v yielded the following expression for frequency of the oscillation

$$f = \frac{kU}{\lambda_v} = \frac{c}{\lambda_A} = \frac{U_\infty}{h} \frac{\left(m_A + m_v - \gamma_v\right)}{\left(M_\infty \dfrac{c}{c_\infty} + \dfrac{1}{k}\right)} \tag{4}$$

where U_∞ is the free-stream velocity and M_∞ is the free-stream Mach number. Here the constant k is the proportion of the free-stream velocity U_∞ at which vortices travel over the cavity.

Rossiter found certain variations to exist in frequencies emitted by cavities of varied length/depth ratio but that the noise generation phenomenon was basically two-dimensional with primary dependence upon h. From measurements of fluid temperature within the cavity, he found c/c_∞ to be essentially 1.0. Finally, a relationship between Strouhal number and Mach number was obtained of the form

$$S = \frac{hf}{U_\infty} = \frac{m_h - \beta}{(M_\infty + 1/k)} \tag{5}$$

with β being a constant and m_h being the sum of the number of complete participating wavelengths of the vortex motion and those of the acoustic radiation.

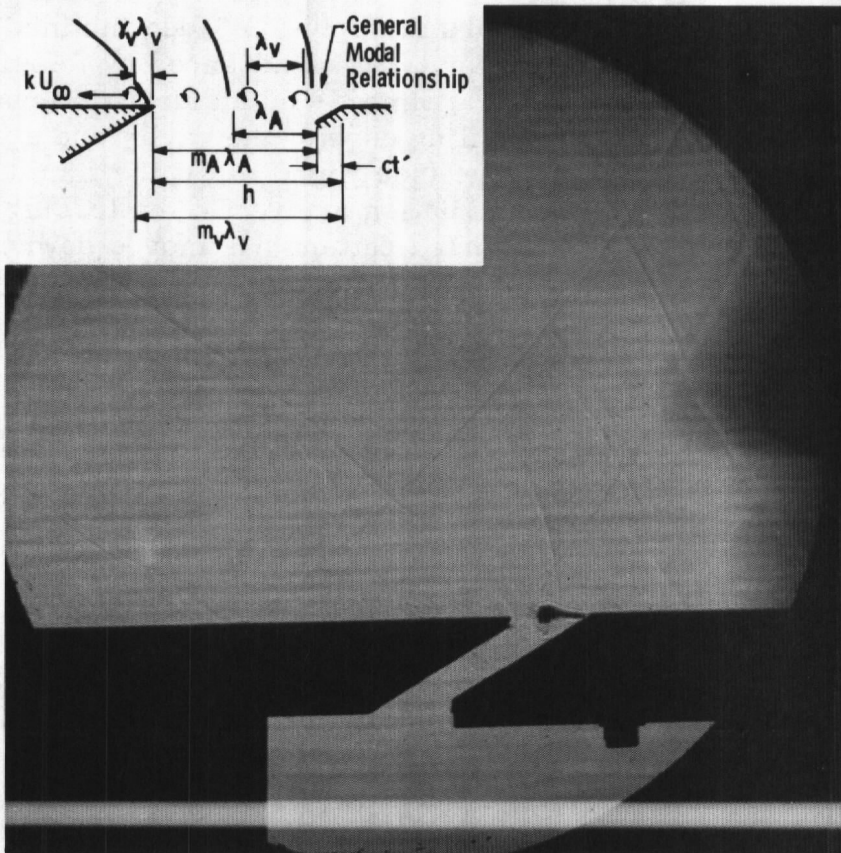Figure 6. Shadowgraph view of vortex over a 60-deg inclined slot ($K_A = 1$ mode).

McCanless (Ref. 2) and Credle (Ref. 15) were able to correlate tone frequency measurements in Tunnels 16T and 4T with the hole size using empirical expressions very similar in form to Eq. (5). McCanless' expression is

$$S = \frac{hf}{U_\infty} = \frac{0.15 \, n^{1.68}}{(M_\infty + 1)} \tag{6}$$

$$n = 1,2,3,4$$

Credle's expression uses a local wall velocity, $\overline{U}_{wall}$, and Mach number, $\overline{M}_{wall}$, to give

$$S = \frac{hf}{\overline{U}_{wall}} = \frac{0.16\, n^{1.55}}{(\overline{M}_{wall} + 0.7)} \tag{7}$$

$$n = 1,2,3,4$$

where he assumed $\overline{U}_{wall}/U_\infty = 0.7$. The frequency measurements from perforated wall samples in the 6-in. ART, however, revealed a harmonic family of frequencies with many more tones than the four which are correlated by Eqs. (6) and (7). From these measurements, a more general expression for Strouhal number was obtained, defining an acoustic wave number, K_A, and noting the empirical constants in Eqs. (6) and (7) to be approximately $1/2\pi$

$$S = \frac{hf}{U_\infty} = \frac{1}{2\pi} \frac{K_A}{(M_\infty + 1)} \tag{8}$$

$$K_A = 1,2,3,\text{------}$$

Predominant noise frequencies measured in Tunnels 1T, 4T, and 16T are seen to be adequately correlated by both Eqs. (6) and (8) in Fig. 7 with coincidence between the following harmonic relationships: $2^{1.68} \approx 3$ and $3^{1.68} \approx 6$. Indeed the $K_A = 1$, 3, and 6 tones are prevalent; but other harmonic multiples are present as well. Recently, McCanless and Boone (Ref. 16) have proposed a more detailed vortex flow model with significantly increased vortex strength because of the shearing that occurs at the trailing edge of a 60-deg inclined hole. This model is also compatible with that derived by Rossiter.

Verification of the vortex hypothesis was obtained from shadowgraph observations of flow over a transverse slot spanning the bottom wall in the 6-in. ART. The view in Fig. 6 was obtained by a simple adjustment of the knife-edge setting in the schlieren system. With the slot gap, h, set at 3/4 in., the vortex described by Rossiter is clearly observed over the two-dimensional 60-deg inclined slot during fundamental, $K_A = 1$, tone generation at Mach number 0.75. A typical schlieren view with the slot gap at 1-1/2 in. (corresponding to the Tunnel 16T wall hole size/plate thickness geometry) is shown in Fig. 8a for sound wave generation in the fundamental mode, $K_A = 1$. (A 1/4-in.-diam 30-deg cone-cylinder model has been placed in the flow

15

to provide unequivocal proof that this is subsonic flow, Mach number 0.75 in this case.) Sound waves from the slot in a higher mode, $K_A = 2$, are shown in Fig. 8b for the 1-1/2-in. gap with plenum suction applied at Mach number 0.75.
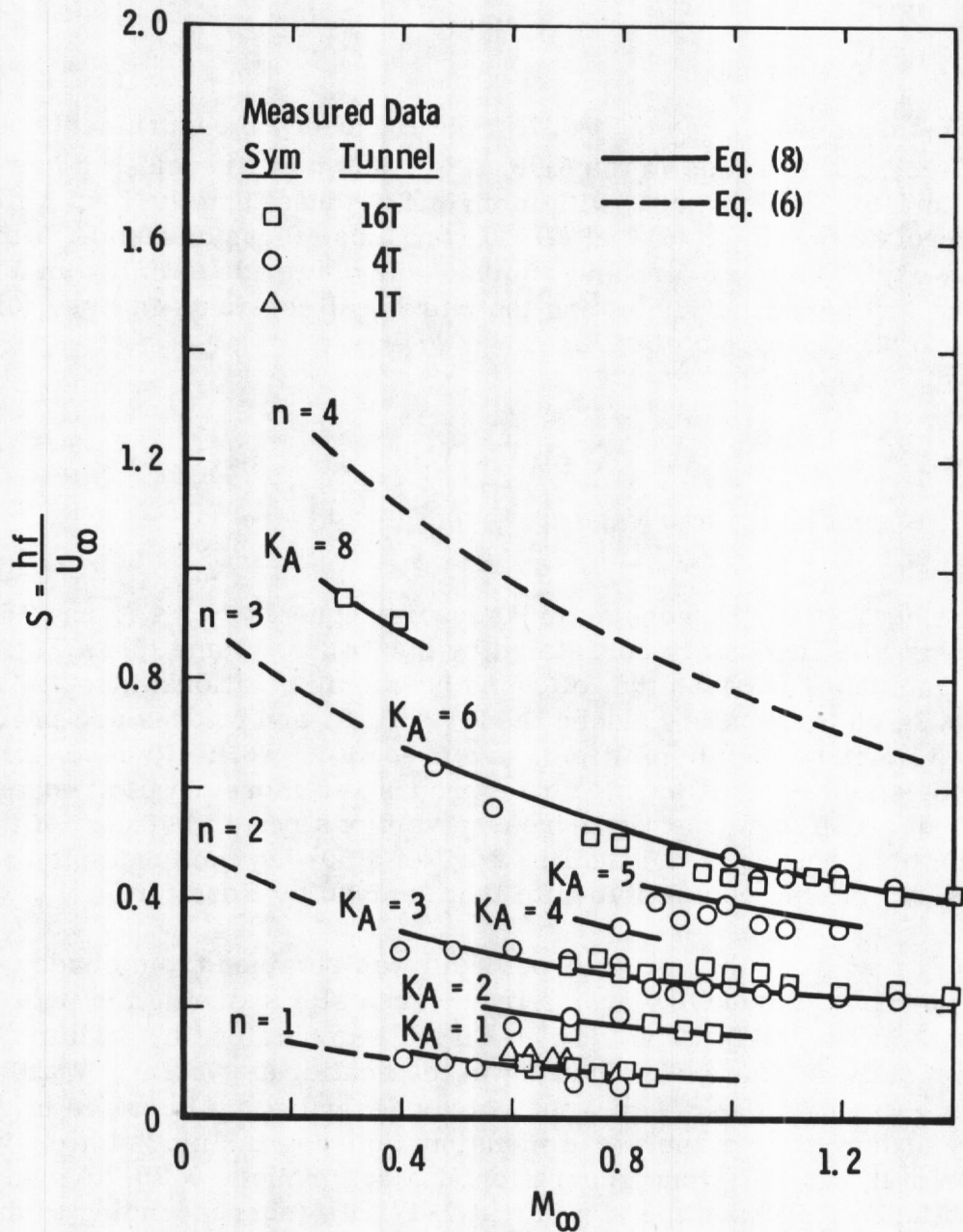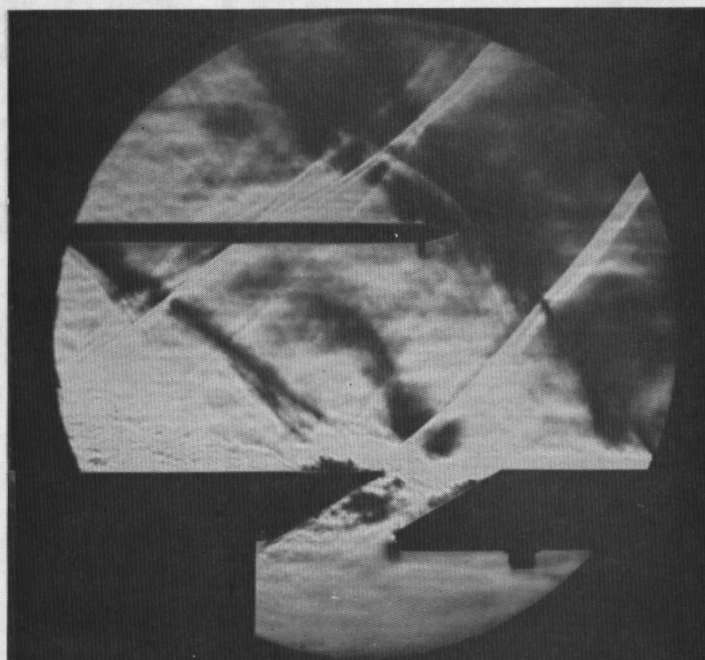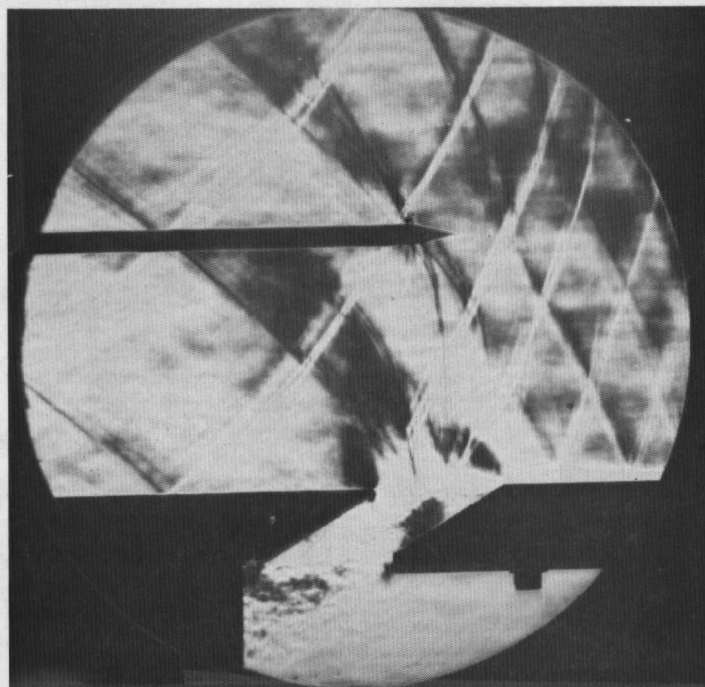

Figure 7. Predominant frequencies measured in Tunnels 16T, 4T, and 1T.

a. Acoustic wave number 1.

b. Acoustic wave number 2
Figure 8. Schlieren views of sound field from slot
with 16T wall cross section.

The theoretical development to this point has been for a single source (hole, slot, or rectangular cavity). The central question for the perforated wall, however, is why the noise mechanism from the array of holes should be correlated by such a simple expression (Eq. 8) based only on a single hole. Schlieren data taken during Tunnel 1T operation, with perforated wall samples installed, revealed regularly spaced uniform wave patterns such as shown in Fig. 9.
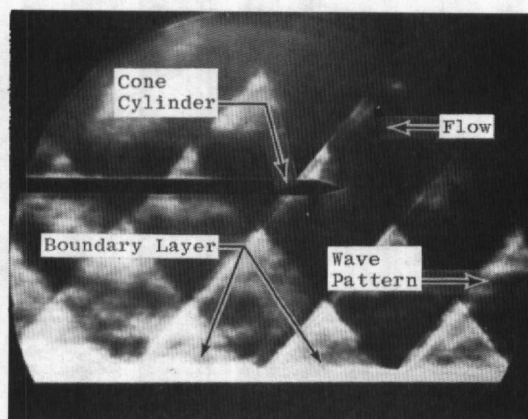
$M_\infty = 0.80$
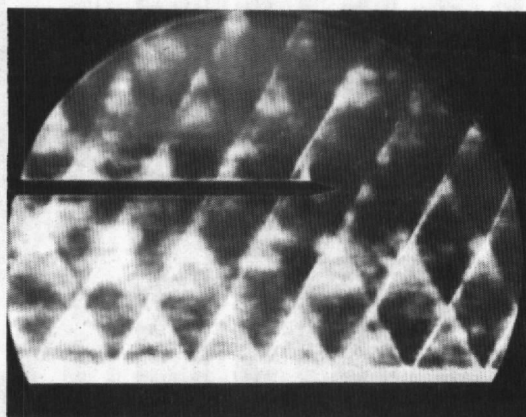
$M_\infty = 0.90$

Figure 9. Schlieren views of sound field from top and bottom pair of Tunnel 1T perforated walls.

These views are typical of wave patterns from the other samples as well, except for the change in acoustic wavelength, λ_A, with the hole size. As Mach number was varied, there was a clear reinforcement of the waves into this diamond pattern where the inclination angle α was observed to obey the following relationship

$$\sin \alpha = M_\infty$$

$$0.5 \leq M_\infty \leq 0.9 \tag{9}$$

The coalesced diamond wave pattern in Fig. 9 clearly indicates a unison behavior from the array of distributed sources, suggesting a boundary condition based upon hole size and a boundary condition based upon hole spacing to be satisfied simultaneously.

For waves inclined at the angle α, a third boundary condition is involved in the wave reinforcement phenomenon. This is the test section cross-sectional dimension, L_x. Expressing the time required for a disturbance to emanate from a wall, travel to the opposing wall, and return yields a natural reverberation frequency

$$fn^2 = \frac{m_x^2 \, c_\infty^2}{4L_x^2} (1 - M_\infty^2) \tag{10}$$

$$m_x = 1,2,3,4,\text{------}$$

after substituting M_∞ for $\sin \alpha$. Here m_x is the number of acoustic wavelengths, λ_A, involved. Varner (Ref. 17) has carried this solution to completion for the distributed sources to include an effective porous zone length dimension with end corrections, L_z. He obtains a simple relationship for a resonant Mach number that

$$M_{\infty_{res}} = \frac{1}{\sqrt{1 + t_r^2 \left(\frac{L_x}{L_z}\right)^2}} \tag{11}$$

where t_r is an odd integer, 1, 3, or 5. Equation (11) has been experimentally verified to hold in Tunnels 1T, 4T, and 16T and for each wall sample in the 6-in. ART. Furthermore, there was a cutoff phenomenon that the fundamental mode, $K_A = 1$, did not occur for either the Tunnel 16T or Tunnel 4T wall samples in the 6-in. ART because the wavelength exceeded the 6-in. cross-sectional dimension of the test section.

While the hole spacing and tunnel size play a significant role in amplifying the sound generation mechanism at each hole and determining which modes of oscillation will appear, the analogy to the classical edgetone focuses upon the interaction between shear layer and sharp

19

trailing edge for the individual hole. Thus, the identification as edge-tones has been aptly applied to the acoustic radiation from 60-deg inclined holes, and the high amplitudes that occur in wind tunnels are the result of acoustic resonance amplification by the test section geometry.

6.0 WALL NOISE SUPPRESSION

Three basic ideas were used as a guide for selecting the hole modifications to be tried. These were that the dynamic feedback loop of vortex interaction could be interrupted and the edgetones thereby suppressed if:

1. Vortex impingement on the hole trailing edge might be prevented,

2. The vortex might be disrupted during its development, or

3. The shear layer might be stabilized such that it could not support the development of the vortex.

A summary of the test configurations investigated is given in Table 2. All of these configurations gave some measure of noise reduction when compared to the standard unmodified wall.

Table 2. Summary of Test Configurations

Code	Name	Tunnel Wall Sample Used		
		16T	4T	1T
1	Standard	x	x	x
2A	Recessed Trailing Edge (Shallow)	x		
2B	Recessed Trailing Edge (Shallow and Blunted)	x		
2C	Recessed Trailing Edge (Deep)			x
3A	Exposed Stud Spoiler (High)	x		
3B	Exposed Stud Spoiler (Low)	x		
3C	Internal Spoiler (Flush)	x	x	
3D	Internal Spoiler (Exposed)	x		
4A	Splitter Plate (Full-Depth)	x		
4B	Splitter Plate (Zero-Depth, Wire)	x		
4C	Splitter Plate (Half-Depth)	x	x	x
5	Backing Tab	x		

The class of configurations denoted as Code 2 followed idea No. 1 above of preventing vortex impingement on the hole trailing edge. Configuration 2A applied to a Tunnel 16T wall sample is shown in Fig. 10.
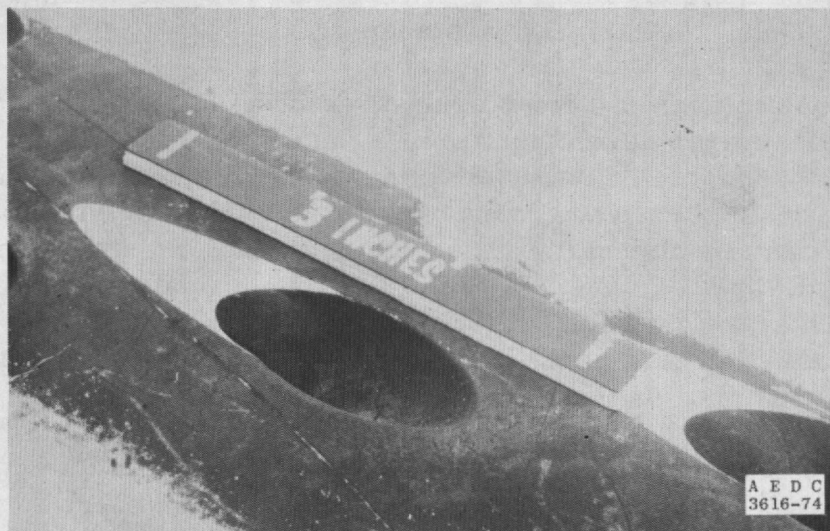

Figure 10. Detail view of recessed trailing-edge configuration in a Tunnel 16T wall sample.

A comparison of measured test section noise levels for Tunnel 16T wall samples with the configuration 2 modifications is shown in Fig. 11.*
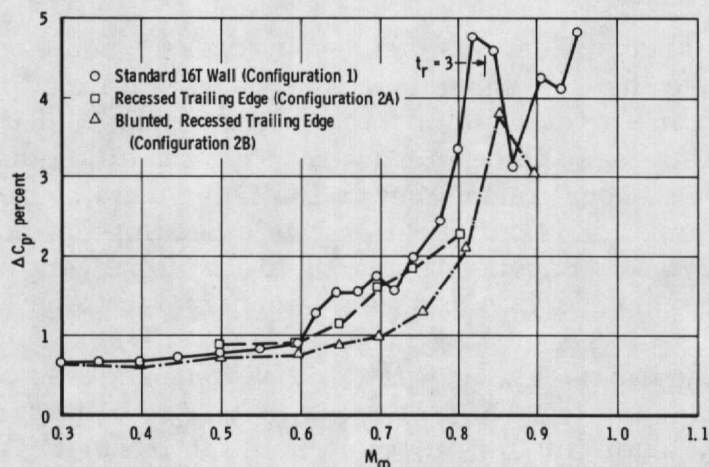

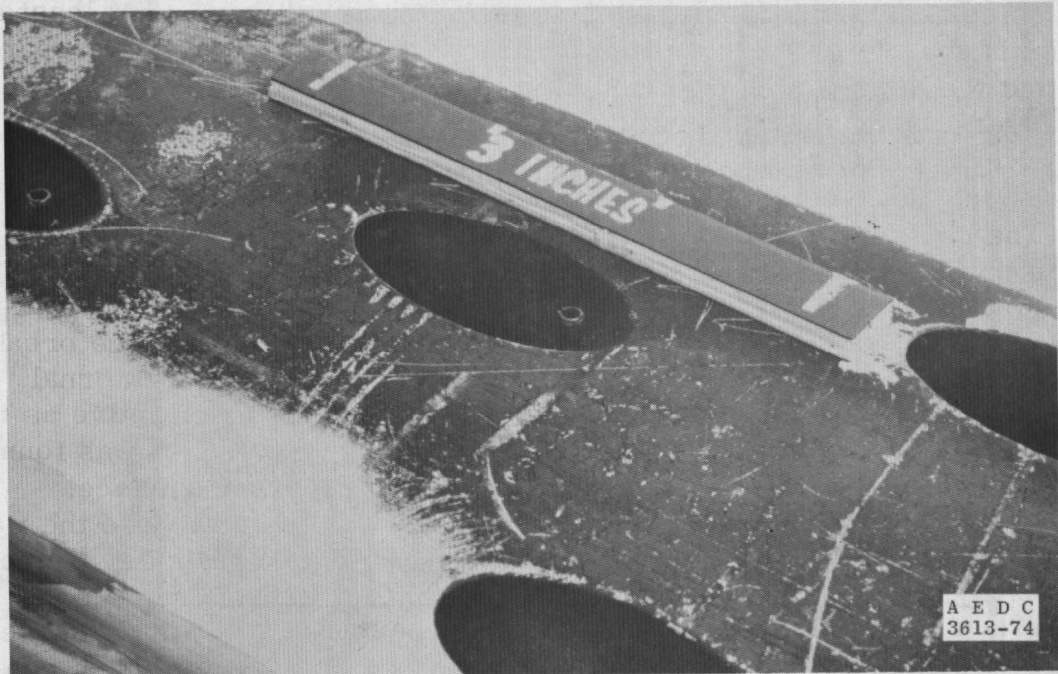**Figure 11. Examples of noise reduction from the recessed trailing edge.**

---

*Data from the plenum microphone are not presented because the principal noise components recorded were the edgetones with no significant contributions from the plenum chamber to the test section.

The noise reduction did not meet the established criterion of at least a factor of three with the recessed trailing edge. It soon became apparent that the degree of recess and blunting that would be required was too severe, with significant change in the basic 60-deg inclined hole geometry. Thus, this scheme was abandoned.

The class of configurations denoted as code 3 followed idea No. 2 above that the vortex development might be disrupted. The idea employed was that a spoiler near the forward edge or within the hole might generate vorticity in a plane transverse to the shear layer, thus breaking up the vortex required for generating an edgetone. The internal spoiler, configuration 3C (Fig. 12a), was found to be as effective as the exposed stud, configuration 3A (Fig. 12b). Furthermore, it was found that the internal spoiler need not protrude above the wall surface. Location of this spoiler (a vertically oriented post** relative to the wall plane) was at the focus of the ellipse from a view perpendicular to the wall. The noise reduction achieved on a Tunnel 16T wall sample is shown in Fig. 13 for flush and 1/16-in. protruding spoilers to be essentially the same. Although the degree of noise reduction for these configurations exceeded a factor of four at Mach numbers in the 0.8 to 0.9 range, the recessed spoiler applied to a Tunnel 4T wall sample exhibited an undesirable sensitivity of tunnel Mach number distribution to wall divergence angle and suction weight flow variations at intermediate porosities of τ = four to six percent.

The class of modifications denoted by codes 4 and 5 were based on idea No. 3 above that the shear layer might be stabilized such that it would not support vortex development. This concept, if it could be implemented, appeared to be more attractive than the other two from the standpoint that local turbulence at the hole would be decreased rather than promoted. Configuration 5 is a backing tab applied to τ = six-percent walls covering approximately 50 percent of the hole from the upstream direction and was demonstrated to be an effective edgetone suppression device in the RAE 3-X 3-Ft Transonic Tunnel at Bedford, England (Ref. 4). It was tried without success on a Tunnel 16T wall sample. This lack of success may have been due to the non-scale boundary layer for 3/4-in.-diam holes in the 6-in. ART. However, the idea was not pursued because a more universal solution was sought, equally applicable to the fixed six-percent porosity Tunnel 16T and to the variable porosity Tunnel 4T.

**The top of each post was filled with epoxy resin to eliminate the possibility of organ-pipe whistling from a hollow post.

a. Internal spoiler, flush
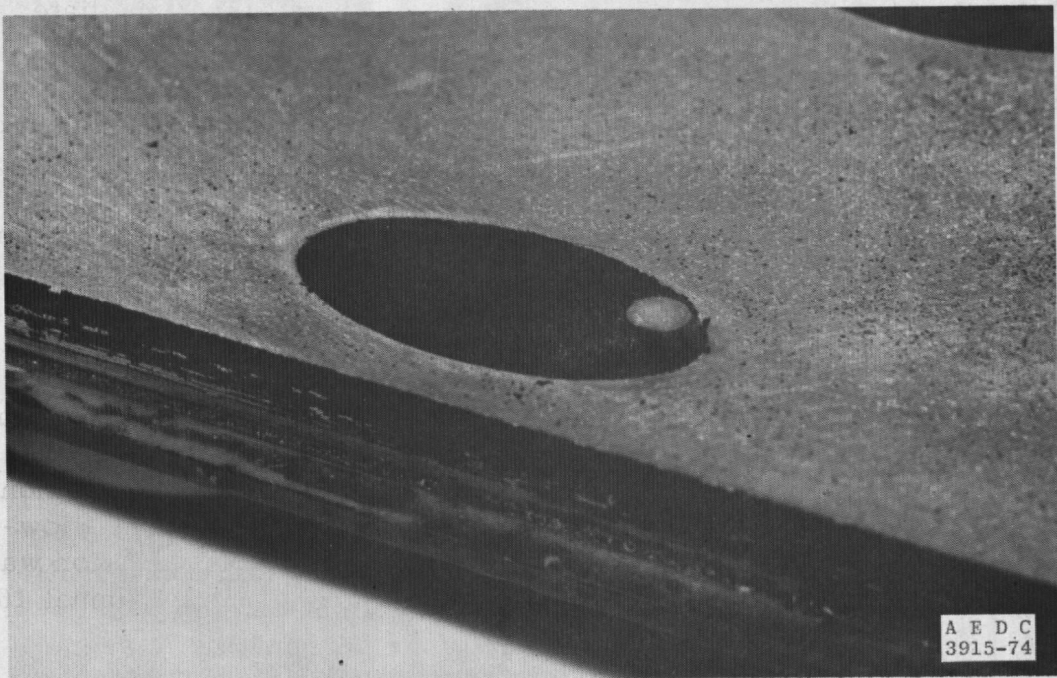
b. Exposed stud, low
Figure 12. Detail views of spoiler configurations in Tunnel 16T wall samples.
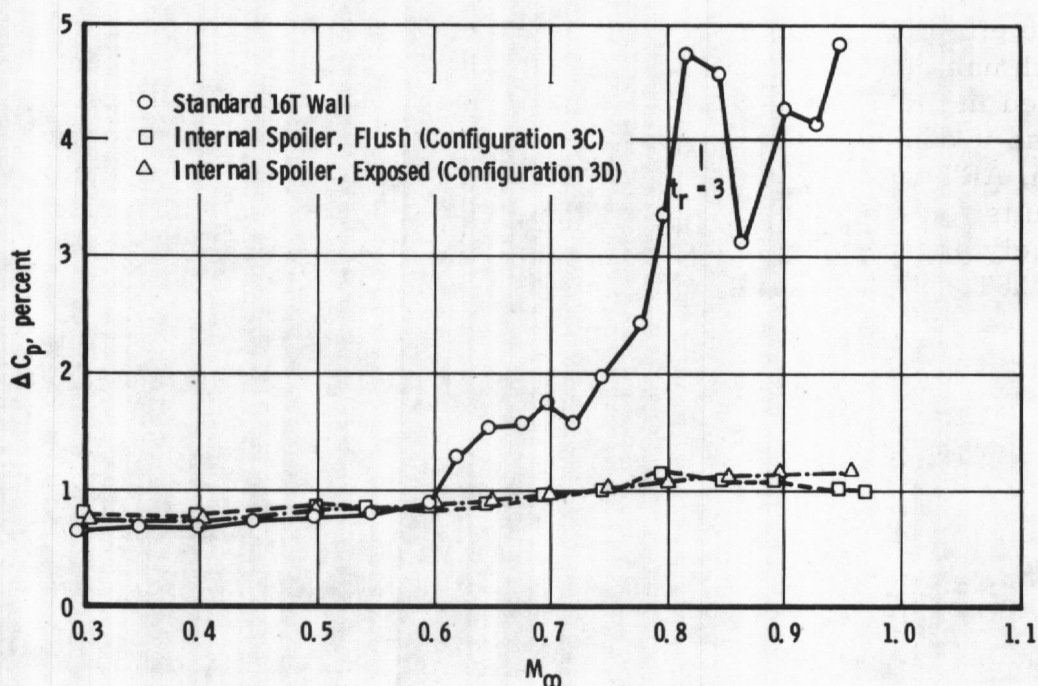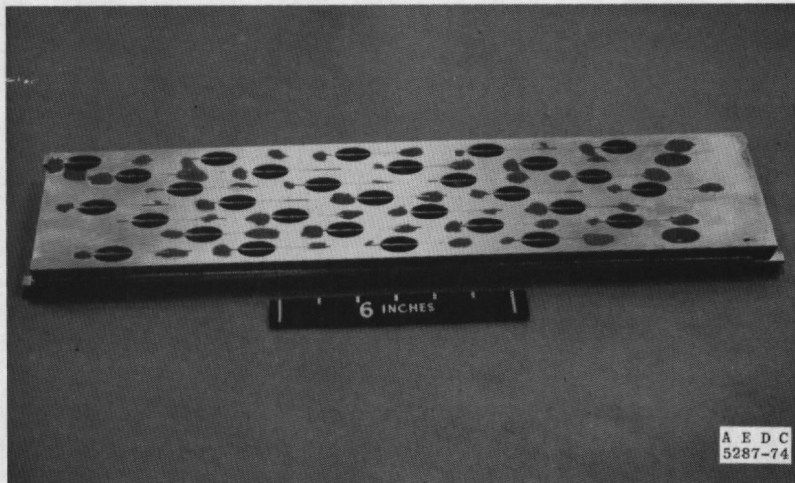
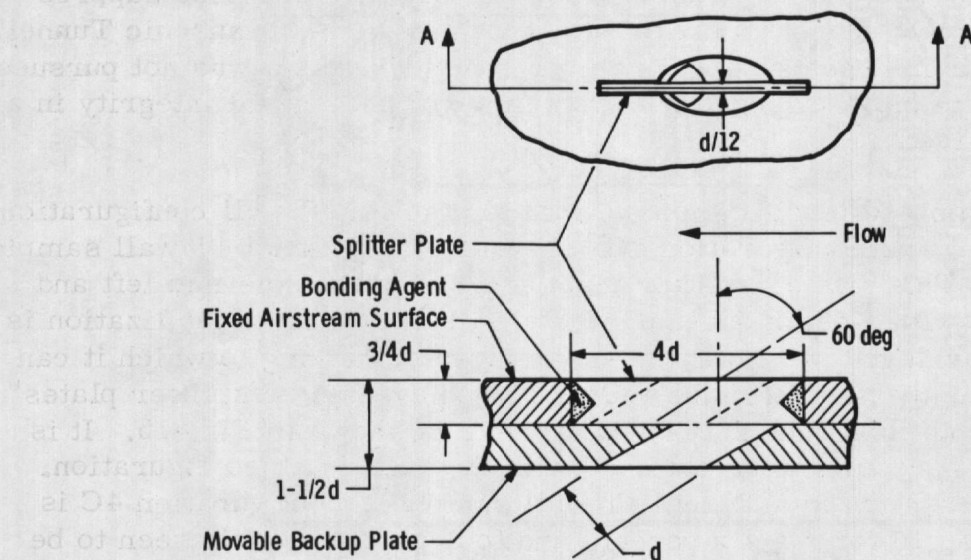**Figure 13.** Examples of noise reduction from internal spoiler configuration in Tunnel 16T wall samples.

One further idea considered that was not tried in these tests was to place wire screen over the holes. This has been demonstrated by Schutzenhofer and Howard (Ref. 18) to give effective edgetone suppression in the NASA/Marshall Space Flight Center 14-in. Transonic Tunnel. The screen idea appears to work as a spoiler device but was not pursued because of anticipated long-term problems with structural integrity in a larger wind tunnel.

The optimized modification scheme for the AEDC wall configurations thus obtained was configuration 4C, shown for the Tunnel 4T wall sample in Fig. 14. This was a "splitter plate", dividing the hole into left and right halves with a depth one-half of the wall thickness. Stabilization is apparently achieved by giving the shear layer something to which it can attach. A comparison of noise reduction achieved with "splitter plates" of varied depth in a Tunnel 16T wall sample is shown in Fig. 15. It is seen that best results were obtained with the half-depth configuration. The noise reduction in a Tunnel 4T wall sample of configuration 4C is shown in Fig. 16 for τ = six percent and four percent and is seen to be about the same as that for the Tunnel 16T wall sample. Finally, the most encouraging result of all was obtained with configuration 4C applied to a Tunnel 1T wall sample as shown in Fig. 17. The resonances

were effectively eliminated with noise reduction by a factor of six at Mach number 0.71. The ΔC_p level of approximately 0.6 percent obtained in the Tunnel 1T wall sample is particularly encouraging because it compares favorably to the 0.45-percent level obtained in the 6-in. ART with solid test section walls and because it shows the best results for a hole size/boundary-layer thickness ratio which more closely approximates the correct ratio for the full-scale Tunnels 4T and 16T.

a. Overall view

b. Cross-sectional view

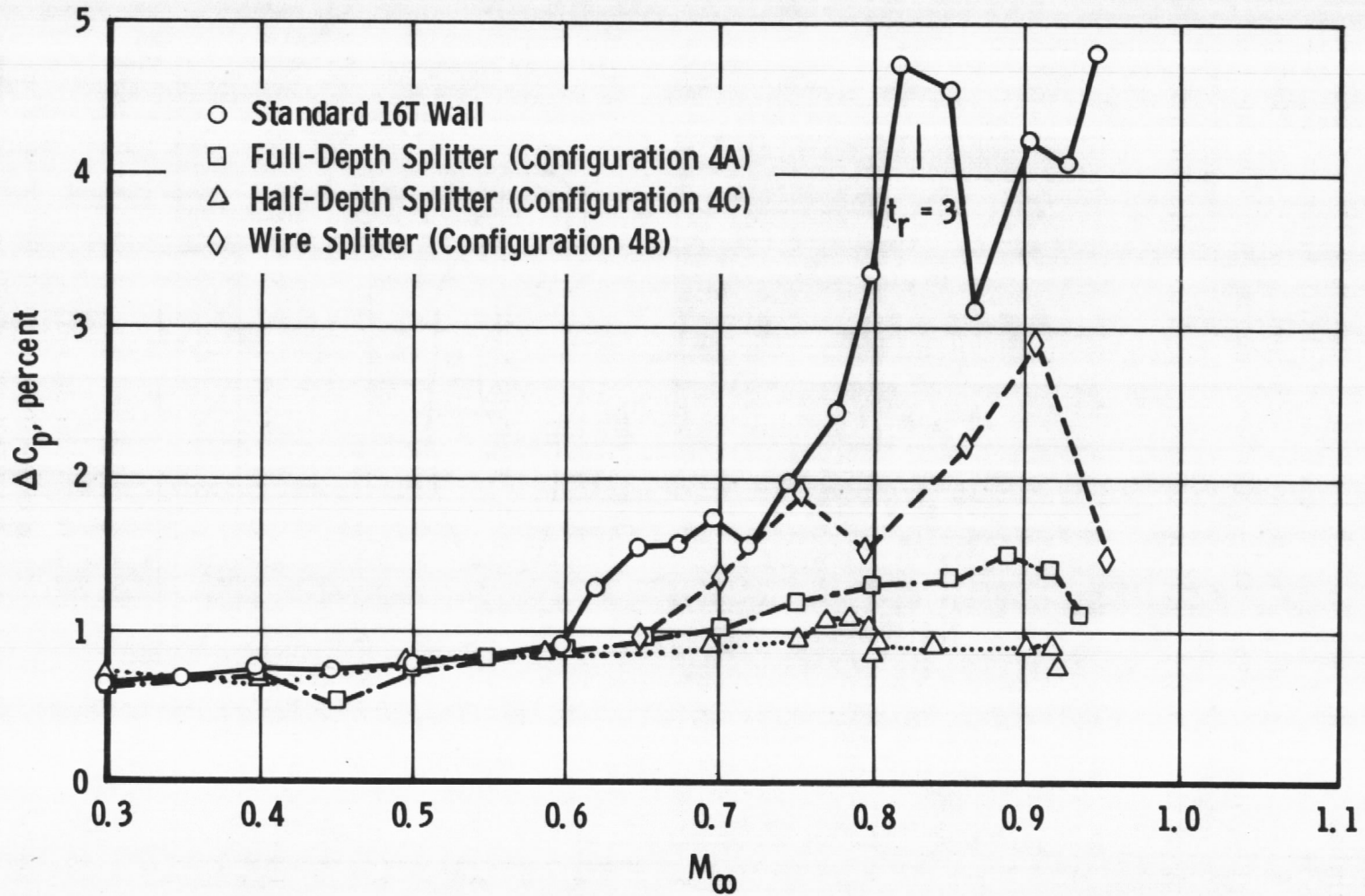Figure 14. Details of the splitter plate configuration in a Tunnel 4T wall sample.

Figure 15. Examples of noise reduction from splitter plate configurations
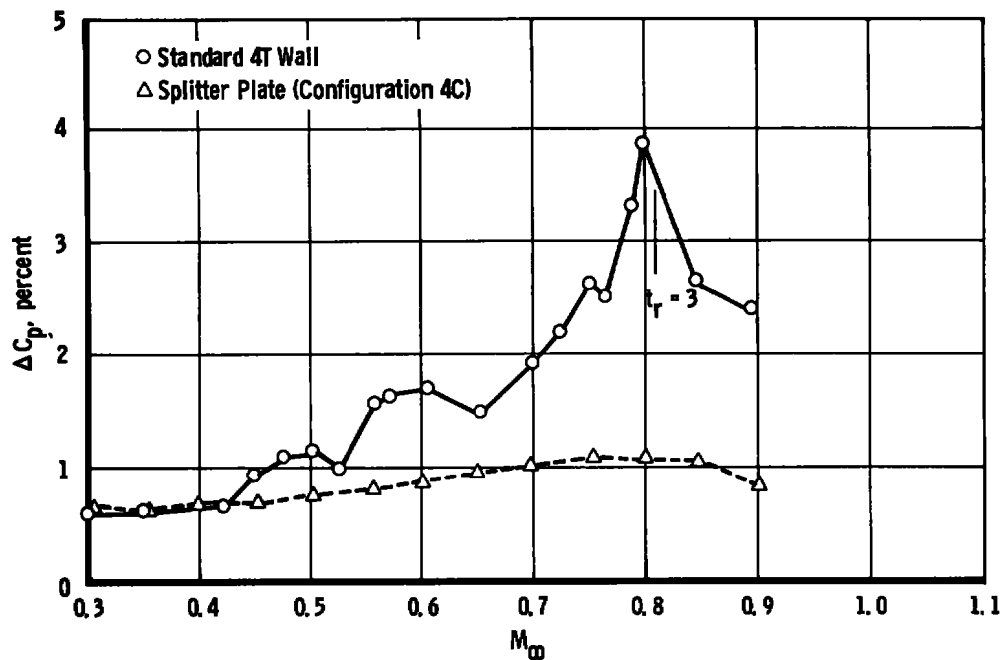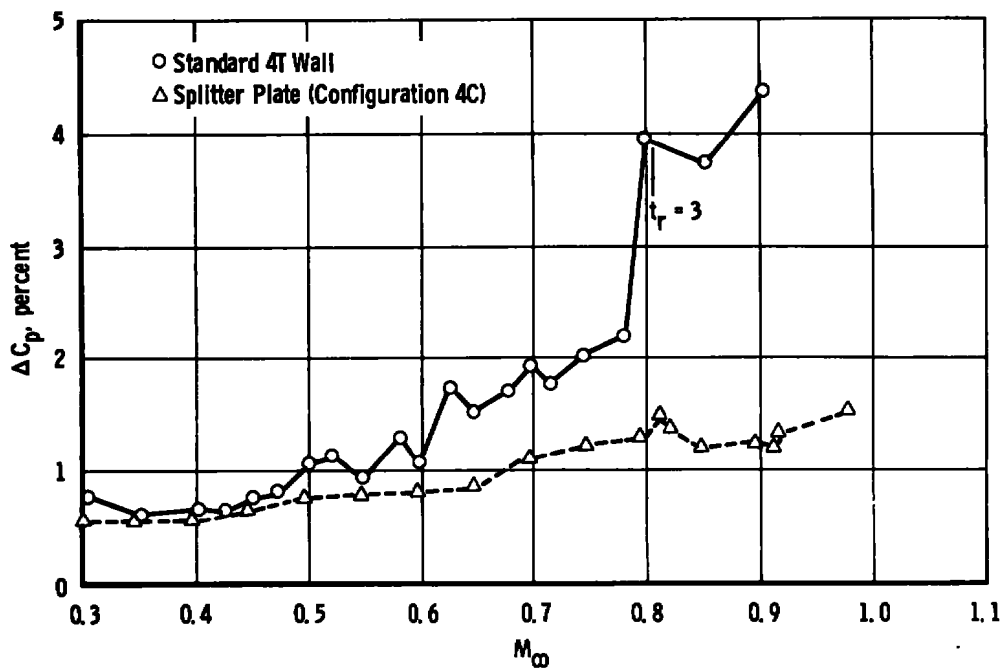in Tunnel 16T wall samples.

a. Porosity τ = six percent

b. Porosity τ = four percent

Figure 16. Examples of noise reduction from splitter plate configuration
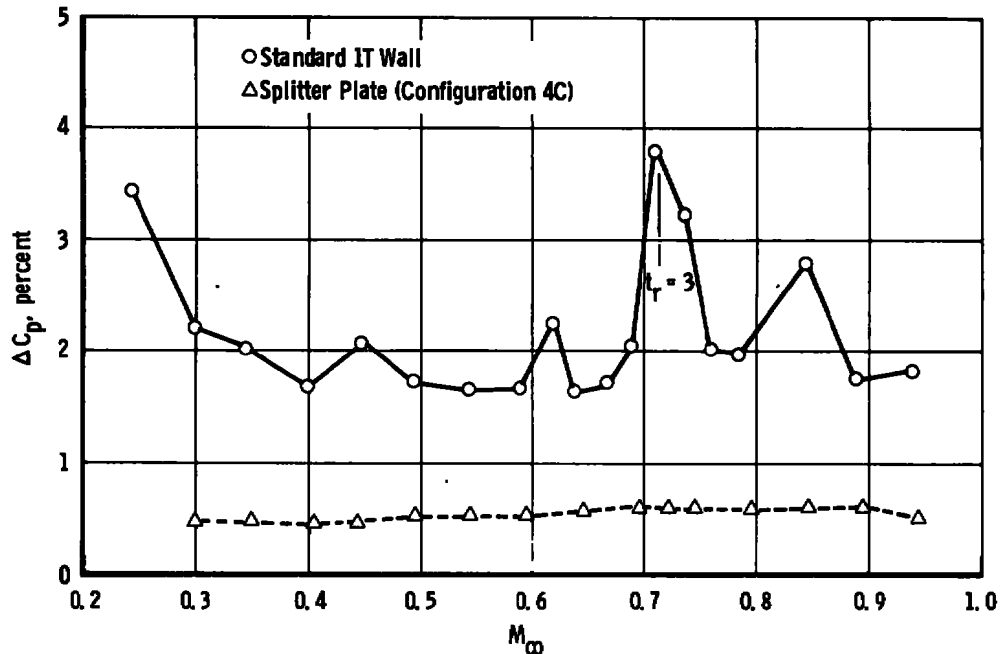in Tunnel 4T variable porosity wall samples.

Figure 17. Noise reduction from splitter plate configuration in a Tunnel 1T wall sample.

7.0 TRANSONIC PERFORMANCE OF THE MODIFIED WALLS

Based upon these test results in the 6-in. ART, the "splitter plate" configuration 4C was chosen for testing in a set of four fully perforated walls in Tunnel 1T. A die was manufactured in order to mass produce the plates.

The noise reduction achieved with this modification in Tunnel 1T is shown in Fig. 18 as indicated by a 1/8-in.-diam Kulite pressure transducer mounted on the test section side wall. These data obtained with properly scaled test hardware prove the feasibility of the technique. The data for the standard wall configuration were taken with top and bottom walls only perforated, side walls solid, and are compared with all four modified walls perforated. This is the reason for slightly higher ΔC_p for the modified walls at Mach numbers from 0.9 to 1.2. At Mach number 1.3 the ΔC_p level is the same in both cases, 0.52 percent. The important difference is at Mach number 0.65 where the $K_A = 1$ edgetone stage had been in resonance at approximately 3500 Hz, raising the ΔC_p level to 5.4 percent. Spectral analysis revealed the

1. 7-percent level of ΔC_p for the modified walls at Mach number 0. 65 to be dominated by noise from the compressor and that the edgetone phenomenon had been effectively suppressed to the tunnel background level.
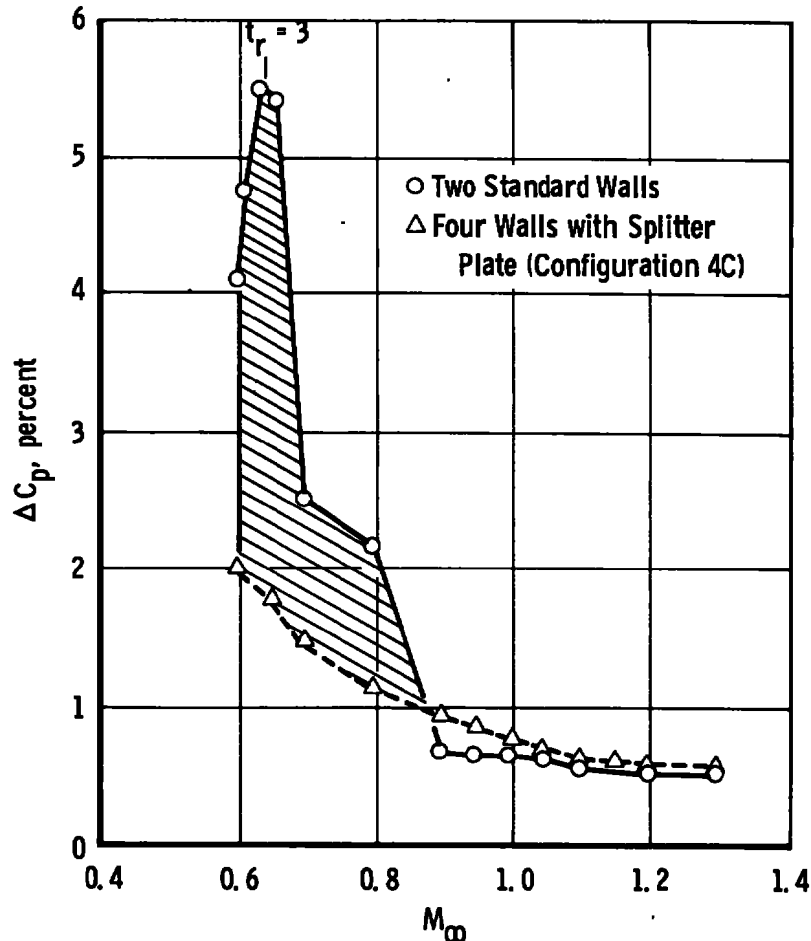
Figure 18. Noise reduction achieved in Tunnel 1T after modifying the perforated walls.

The effect of the modification on the crossflow characteristics of the wall were evaluated by comparing pressure data at matched test conditions on the following: (1) a center-line static pipe (i. e. , for indication of the empty tunnel axial Mach number distribution using previously established tunnel calibrations), (2) a 20-deg cone-cylinder model of two-percent blockage (which generates strong bow shock and shoulder expansion waves to be cancelled at the wall), and (3) a wing-tail lifting model of one-percent blockage (with large regions of

supercritical flow at transonic speeds such that interference from the walls alters the lift coefficient and pitching moment).

Comparison of the centerline static pipe data revealed the 2σ standard deviation in local Mach number through the test section to be as good as or better than that with the original walls at Mach number settings from 0.6 to 1.3. Most importantly, there was no shift in mean Mach number using the previously prescribed schedule for plenum chamber pressure and wall angle. A comprehensive comparison of the flow generation properties of the two wall configurations is given in Ref. 19.

Pressure distributions on the 20-deg cone-cylinder model are shown in Fig. 19. for the modified and standard wall in comparison with a
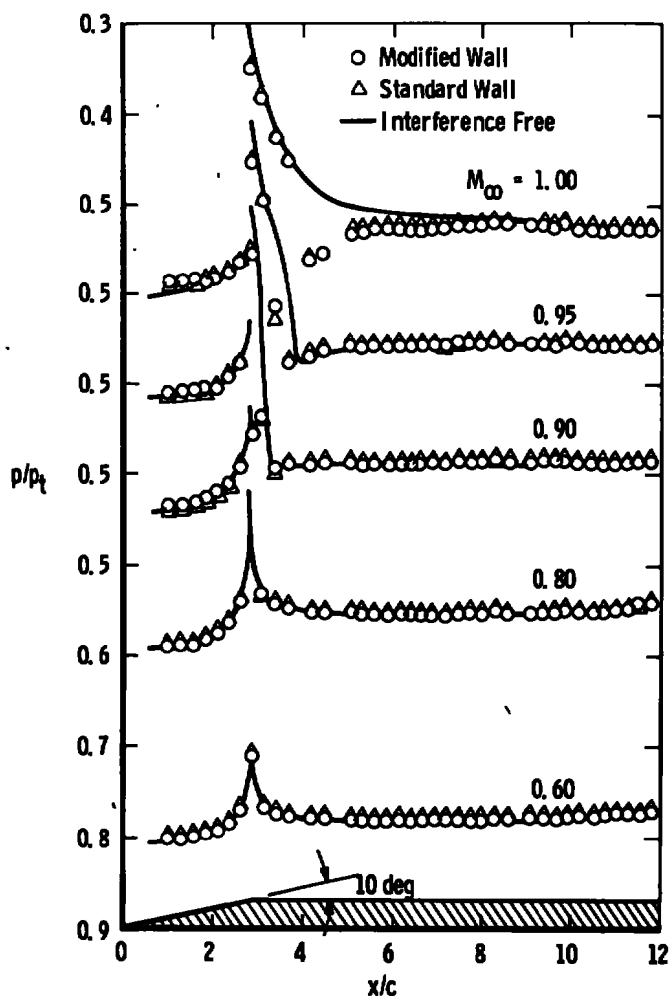
Figure 19. Comparison of pressure distributions on the 20-deg cone-cylinder in Tunnel 1T.

30
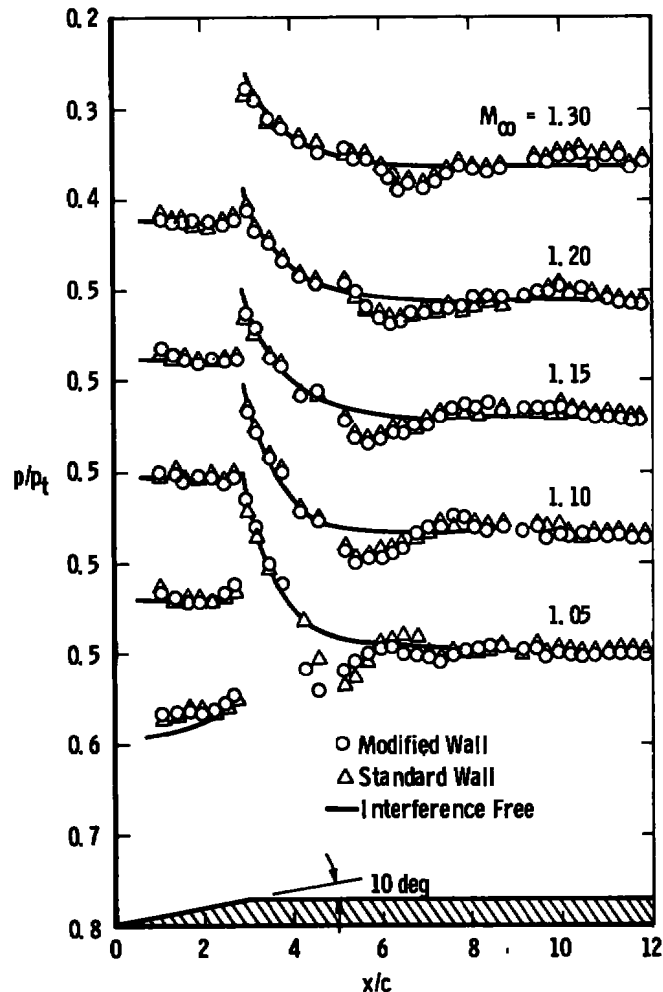
Figure 19. Concluded.

theoretical free-air solution given by the Douglas-Neumann computer program (Ref. 20). Deviations in pressure distribution from interference-free trends at Mach numbers between 1.0 and 1.15 are attributable to impingement of the bow shock reflected as an expansion wave from the walls. Better agreement with the interference-free solution occurred when the Mach number was increased to 1.2 and 1.3 as the perforations give better attenuation of the model-generated waves at these Mach numbers. As seen in Fig. 19, there was no appreciable difference between the standard and the modified walls in these tests over the full Mach number range considered.

Finally, typical pressure coefficient data, C_p, over both wing and tail upper surfaces of the lifting model are shown in Fig. 20 over the range of Mach numbers where transonic flow occurs on the model. Except for slight rearward shift in shock locations at Mach number 0.95, there was no appreciable difference in these data with the modified and standard wall.

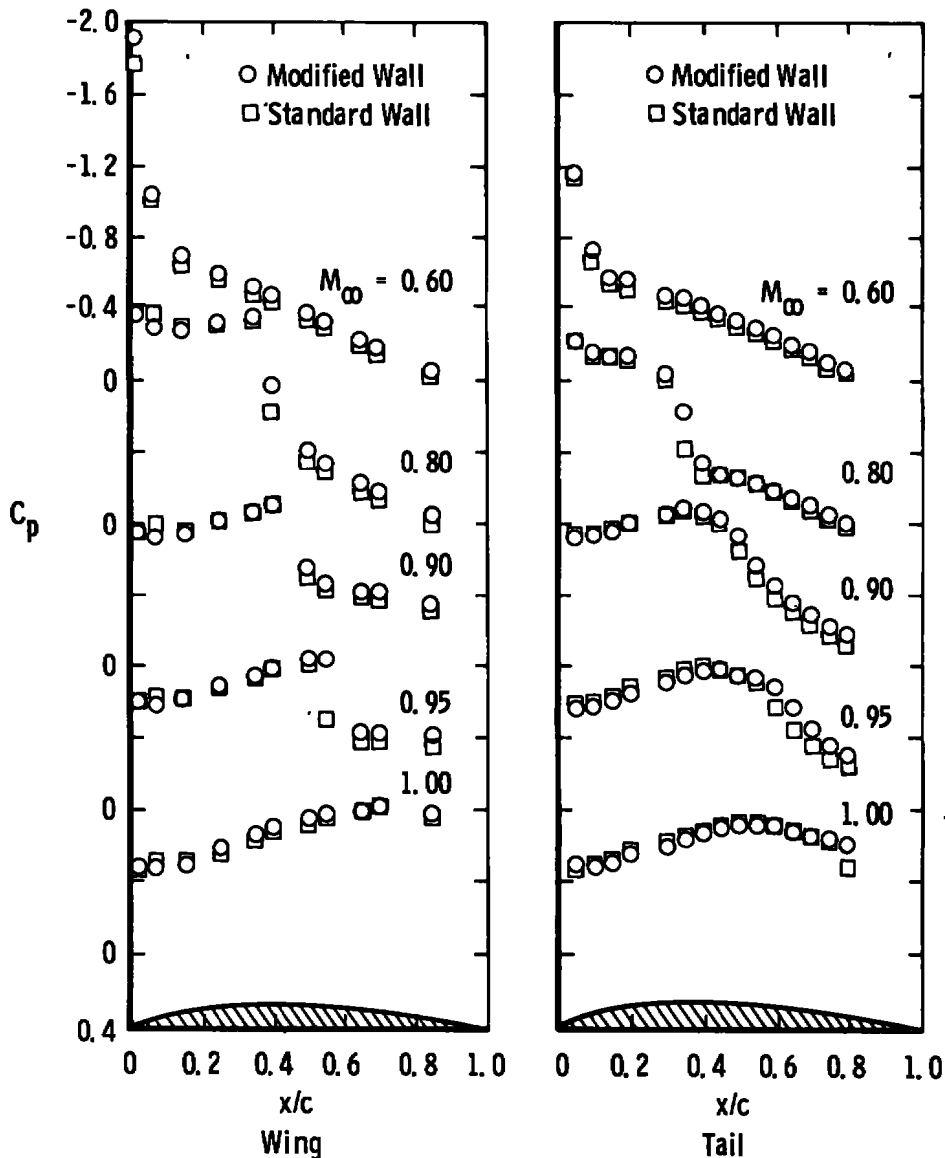Figure 20. Comparison of pressure distributions on the wing-tail lifting model in Tunnel 1T.

8.0 CONCLUSIONS

The primary conclusions from this investigation are as follows:

1. The "splitter plate" modification has been demonstrated to be an effective means of suppressing edgetones from this type of perforated wall with 10 db or more reduction in overall test section noise level at worst-case resonance conditions in the fixed and variable porosity wall samples tested in the 6-In. Acoustic Research Tunnel.

2. This modification has been applied to existing six-percent perforated walls (~8,000 holes) with resonable economy in the 1-Ft Transonic Model Tunnel at AEDC and yielded the desired 10-db noise reduction at resonance demonstrating "proof-of-principle" in properly scaled test hardware.

3. Pressure data acquired on a centerline static pipe, a cone-cylinder model, and a wing-tail lifting model in the 1-Ft Transonic Model Tunnel all indicate that the crossflow characteristics of the modified low-noise, six-percent walls are essentially the same as the original walls.

REFERENCES

1. Cox, R. N. and Freestone, M. M. "Design of Ventilated Walls with Special Emphasis on the Aspect of Noise Generation." Fluid Motion Problems in Wind Tunnel Design. AGARD Report No. 602, No. 6, November 1972.

2. McCanless, G. F. "Additional Correction of 4% Saturn V Protuberance Test Data." Chrysler Corp. TR HSM-R1-71, January 1971.

3. Dods, J. B. and Hanly, R. D. "Evaluation of Transonic and Supersonic Wind Tunnel Background Noise and Effects on Surface Pressure Fluctuation Measurements." AIAA Paper No. 72-1004, presented at the AIAA 7th Aerodynamic Testing Conference, Palo Alto, California, September 1972.

4. Mabey, D. G. "Flow Unsteadiness and Model Vibration in Wind Tunnels at Subsonic and Transonic Speeds." RAE, Bedford, England, CP No. 1155, October 1970.

5. Dougherty, N. S., Jr., and Steinle, F. W., Jr. "Transition Reynolds Number Comparisons in Several Major Transonic Tunnels." AIAA Paper No. 74-627, presented at the AIAA 8th Aerodynamic Testing Conference, Bethesda, Maryland, July 8-10, 1974.

6. Curle, N. "The Mechanics of Edgetones." Proceedings of the Royal Society, England, Vol. 216, p. 416, 1953.

7. Karamcheti, K. "Sound Radiation from Surface Cutouts in High Speed Flow." Ph. D. Thesis, California Institute of Technology, 1956.

8. Pindzola, M. and Chew, W. L. "A Summary of Perforated Wall Wind Tunnel Studies at the Arnold Engineering Development Center." AEDC-TR-60-9 (AD241573), August 1960.

9. Goethert, B. H. Transonic Wind Tunnel Testing. AGARDograph No. 49, Pergamon Press, 1961.

10. Lukasiewicz, J. "Effects of Boundary Layer and Geometry on Characteristics of Perforated Walls for Transonic Wind Tunnels." Aerospace Engineering. Vol. 20, No. 4, April 1961.

11. Jacocks, J. L. "Evaluation of Interference Effects on a Lifting Model in the AEDC-PWT-4-Ft Transonic Tunnel." AEDC-TR-70-72 (AD868290), April 1970.

12. Lowson, M. V. "Prediction of Boundary Layer Pressure Fluctuations." AFFDL-TR-67-167 (AD832715), April 1966.

13. Woolley, J. P. and Karamcheti, K. "A Study of Narrow Band Noise Generation by Flow over Ventilated Walls in Transonic Wind Tunnels." AFOSR-TR-73-0503 (AD758254), February 1973.

14. Rossiter, J. E. "Wind-Tunnel Experiments on the Flow over Rectangular Cavities at Subsonic and Transonic Speeds." Aeronautical Research Council, London, England, Reports and Memoranda No. 3438, October 1964.

15. Credle, O. P. "Perforated Wall Noise in the AEDC-PWT 16-Ft and 4-Ft Transonic Tunnels." AEDC-TR-71-216 (AD888561L), October 1971.

16. McCanless, G. F., and Boone, J. R. "Noise Reduction in Transonic Wind Tunnels." Journal of the Acoustical Society of America, Vol. 56. No. 5, November 1974.

17. Varner, M. O. "Noise Generation in Transonic Tunnels." AIAA Paper No. 74-633, presented at the AIAA 8th Aerodynamic Testing Conference, Bethesda, Maryland, July 8-10, 1974.

18. Schutzenhofer, L. A. and Howard, P. W. "Suppression of Background Noise in MSFC 14-in. Transonic Wind Tunnel Test Section." Fall 1974 Research Technology Review, NASA/ Marshall Space Flight Center, Huntsville, Alabama, October 1974.

19. Parker, R. L., Jr. "Flow Generation Properties of Five Transonic Wind Tunnel Test Section Wall Configurations." AEDC-TR-75-73, 1975.

20. Smith, A. M. O. and Pierce, Jesse. "Exact Solution of the Neumann Problem. Calculation of Non-Circulatory Plane and Axially Symmetric Flows About or Within Arbitrary Boundaries." Douglas Aircraft Company. Report No. ES 26988 (AD161445), April, 1958.

NOMENCLATURE

C_p	Pressure coefficient, $(p - p_\infty)/q_\infty$
ΔC_p	Fluctuating pressure coefficient, Eq. (1), percent
c	Local speed of sound, ft/sec
c_∞	Free-stream speed of sound, ft/sec
f	Frequency, Hz
f_n	Natural reverberation frequency, Hz, Eq. (10)
h	Axial distance between leading and trailing edges of perforations or cavities, ft
K_A	Acoustic wave number, 1,2,3,4,------
k	Proportion of free-stream velocity at which vortices travel over cavity
L_x	Cross-sectional dimension of test section, ft
L_z	Effective length of test section porous zone, ft
M_∞	Free-stream Mach number
$M_{\infty res}$	Resonant free-stream Mach number, Eq. (11)
$\overline{M}_{wall}$	Local Mach number evaluated near the wall
m_A	Number of acoustic wavelengths passing over cavity per cycle
m_h	Total number of acoustic and vorticity wavelengths per cycle, $m_A + m_V$
m_V	Number of vorticity wavelengths passing over cavity per cycle
m_x	Number of acoustic wavelengths across the test section per cycle
n	Edgetone stage 1,2,3, or 4, Eqs. (6) and (7)
p	Mean local static pressure, psfa
p_t	Stagnation pressure, psfa
p_∞	Free-stream static pressure, psfa

$\tilde{P}_{rms}$	Fluctuating pressure, root-mean-square time-averaged, frequency-integrated, psf
q_∞	Free-stream dynamic pressure, psf
Re/ft	Unit Reynolds number per foot based on free-stream conditions
S	Strouhal number, nondimensionalized frequency
t	Time, sec
t'	Specified instant of time, sec
t_r	An odd integer, 1, 3, 5, 7, -----
U	Local velocity in the boundary layer, ft/sec
U_∞	Free-stream mean velocity, ft/sec
$\overline{U}_{wall}$	Average local velocity near the wall, ft/sec
x/c	Body-axis position normalized to overall length or to chord length
α	Inclination angle of plane sound waves relative to free-stream flow axis, deg, Eq. (9)
β	An empirical constant, Eq. (5)
γ_v	Scale length constant for vortex positioning
δ	Boundary-layer thickness (to 99 percent of free-stream velocity), in.
δ^*	Boundary-layer displacement thickness, in.
λ_A	Acoustic wavelength, ft
λ_v	Axial spacing of vortices, ft
σ	Standard deviation
τ	Porosity, the ratio of open area/total area of the wall sample, percent